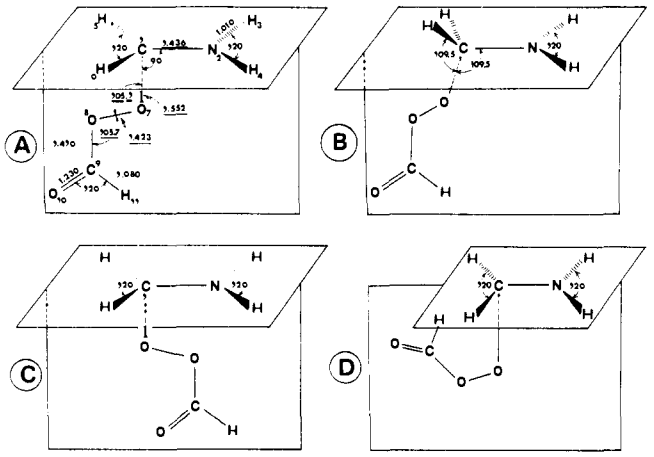

Figure 4. The geometries of adducts A–D. Underlined values are optimized.

metric arrangements (A, C, D) were investigated (Figure 4). Fairly extensive minimization was performed only in the case of conformation A, which has been found to possess the lowest energy. A considerably more stable conformation **B** resulted from the relaxation of the carbon atom to the tetrahedral one. **B** lies 36.3 kcal/mol below reactants and 17.5 kcal/mol below products. These results seem to support the experimental evidence which has been accumulated recently in favor of the two-step mechanism with the addition of peroxy acid to C=N of acyclic imines being the rate-determining step,[4,10-12] It seems quite probable that the transition state for the formation of the adduct resembles the one represented as **4** (reactant-like). The transition state for the second step (intramolecular nucleophilic reaction) is expected to be more product-like. The fact that an aliphatic imine reacts with hydrogen peroxide to form an adduct which is easily converted to an oxaziridine on gentle heating is also in accordance with the above-mentioned results.[13]

Acknowledgment. The authors wish to thank the Boris Kidrič Fund for the financial support of this research.

References and Notes

(1) W. D. Emmons, *J. Am. Chem. Soc.*, **79**, 5739 (1957).
(2) V. Madan and L. B. Clapp, *J. Am. Chem. Soc.*, **91**, 6078 (1969); **92**, 4902 (1970).
(3) E. Schmitz, R. Ohme, and D. Murawski, *Chem. Ber.*, **98**, 2516 (1965).
(4) Y. Ogata and Y. Sawaki, *J. Am. Chem. Soc.*, **95**, 4687, 4692 (1973).
(5) W. J. Hehre, R. F. Stewart, and J. A. Pople, *J. Chem. Phys.*, **51**, 2657 (1969).
(6) B. Plesničar, M. Tasevski, and A. Ažman, *J. Am. Chem. Soc.*, **100**, 743 (1978).
(7) The last two values were not optimized; nevertheless, the positive charge on the hydrogens decreases in the order $H_3 > H_5 > H_4$, which is the same as in the completely optimized structure (J. M. Howell, *J. Am. Chem. Soc.*, **98**, 886 (1976); N. D. Epiotis, R. L. Yates, J. R. Larson, C. R. Kirmaier, and F. Bernardi, *ibid.*, **99**, 8379 (1977)).
(8) The term "transition state" is used throughout the paper rather loosely. Arbitrarily chosen molecular arrangements **1–6**, believed to be near the transition state, were selected on the grounds of chemical intuition and probably do not have zero gradient and only one negative force constant for molecular motion (J. W. McIver, Jr., and A. Komornicki, *J. Am. Chem. Soc.*, **94**, 2625 (1972); J. W. McIver, Jr., *Acc. Chem. Res.*, **7**, 72 (1974)).
(9) After completing this study we have optimized also the C–N distance of the transition state **1** and found, in accordance with the results of our previous study of the epoxidation reaction, that it becomes slightly longer as compared to free imine (1.288 Å).
(10) C. Bełzecki and D. Mostowicz, *J. Org. Chem.*, **40**, 3878 (1975).
(11) D. R. Boyd, D. C. Neil, C. G. Watson, and W. B. Jennings, *J. Chem. Soc., Perkin Trans. 2*, 1813 (1975).
(12) M. Bucciarelli, A. Forni, I. Moretti, and G. Torre, *J. Chem. Soc., Perkin Trans. 2*, 1339 (1977).
(13) E. Höft and A. Rieche, *Angew. Chem.*, **77**, 548 (1965).

The 147-nm Photolysis of Monosilane[1]

G. G. A. Perkins, E. R. Austin, and F. W. Lampe*

Contribution from the Davey Laboratory, Department of Chemistry, The Pennsylvania State University, University Park, Pennsylvania 16802. *Received July 18, 1978*

Abstract: The 147-nm photolysis of SiH_4 results in the formation of H_2, Si_2H_6, Si_3H_8, and a solid hydridic silicon film. Two primary processes are involved, namely, (a) $SiH_4 + h\nu \rightarrow SiH_2 + 2H$ and (b) $SiH_4 + h\nu \rightarrow SiH_3 + H$, with $\phi_a = 0.83$ and $\phi_b = 0.17$. The quantum yields depend on the pressure of SiH_4 but at 2 Torr are $\Phi(-SiH_4) = 4.4 \pm 0.6$, $\Phi(Si_2H_6) = 1.29 \pm 0.08$, $\Phi(Si_3H_8) = 0.46 \pm 0.01$, and $\Phi(Si_{wall}) = 0.5$; the quantum yields for H_2 formation were not measured. A mechanism is proposed, which incorporates the known reactions of SiH_2 and SiH_3 radicals, and is shown to be in accord with the experimental facts.

Direct photochemical decomposition of silicon hydrides can occur only for light of wavelength less than 200 nm. While the vacuum ultraviolet photochemistry of methylsilane[2,3] and dimethylsilane[4] has been studied in some detail, only a brief report of the direct photolysis of monosilane,[5] the simplest member of the series, has appeared in the literature.

The $Hg(^3P_1)$-photosensitized decompositions of monosilane[6-10] and the methylsilanes[9] occur predominantly through the formation and subsequent reaction of monovalent silyl radicals, reactions that apparently are more complex in monosilane[9,11,12] than in the methylsilanes.[9] Since the vacuum ultraviolet photolysis of the methylsilanes results mainly in the formation of divalent silylene radicals,[2-4] one may expect the direct photolysis of monosilane to be quite different from the photosensitized decomposition.

As part of a general program concerned with the radiation and photochemical decomposition of gaseous silicon and germanium hydrides, we have studied the 147-nm photolysis of monosilane at 305 K. This paper is a report of our results.

Experimental Section

The photolyses were carried out in a cylindrical cell that had a diameter of 1.9 cm and a length of 13.4 cm. One end of the photolysis cell contained a pinhole leak, with a diameter of 2×10^{-3} cm, that led directly into the ionization region of a time of flight mass spectrometer. The opposite end of the cell was a lithium fluoride window that was common to both the photolysis cell and the light source. The cell was connected via ¼-in. stainless steel and 6-mm Pyrex tubing to large reservoirs containing the reactant gases.

The light source was a xenon resonance lamp in which resonance radiation at 147 (98%) and 130 nm (2%) was produced in an elec-

0002-7863/79/1501-1109$01.00/0

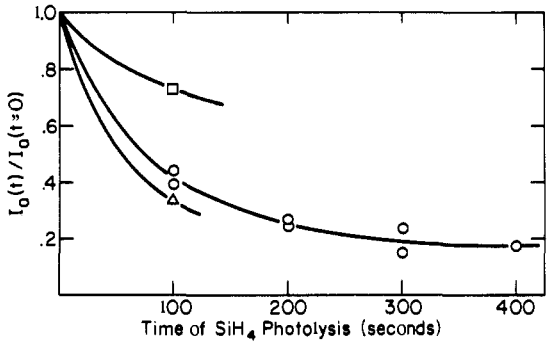

Figure 1. Reduction of incident light intensity by the formation of the film of silicon hydride on the window of the photolysis cell: □, $P(SiH_4)$ = 1 Torr; ○, $P(SiH_4)$ = 2.1 Torr; △; $P(SiH_4)$ = 4 Torr.

trodeless discharge powered by a 2450-MHz microwave generator. The lamp was identical with those described by Gorden, Rebbert, and Ausloos[13] with the exception that the lithium fluoride window was sealed to the rim of the discharge tube by epoxy cement. After prolonged evacuation and degassing on a mercury-free high-vacuum system, the lamp was filled with 0.7 Torr of xenon, as measured with a calibrated Pirani gauge. The light intensity incident on the reactant mixture was determined by several actinometers, namely, CO_2, N_2O, and $(CF_3)_2CO$, for which the quantum yields are $\Phi(-CO_2)$ = 1.0,[14-19] $\Phi(-N_2O)$ = 1.7,[20-23] $\Phi(C_2F_6)$ from $(CF_3)_2CO$ = 1.11 at 4 Torr.[24] Light intensities determined by the various actinometers agreed within ±5%. The actual intensity incident on a reaction mixture through a freshly cleaned window was $2.3 \pm 0.2 \times 10^{15}$ quanta/s.

The vacuum ultraviolet absorption spectrum has been reported by Harada, Murrel, and Sheena.[25] The absorption onset occurs at about 165 nm with the absorbance increasing with decreasing wavelength to a maximum at 114 nm. The extinction coefficients at 114 and 147 nm are 22×10^3 and 4×10^3 L mol^{-1} cm^{-1}, respectively. The spectrum is very similar to that of CH_4, which exhibits an onset at 144 nm and a maximum at 127 nm.[26] The spectral transitions are not known but it has been presumed[27] that the onset and first maximum in CH_4 are due to excitation of a σ electron to a σ^* nonbonding orbital and it is likely that the same type of transition occurs in SiH_4.

The photodecomposition of SiH_4 results in a deposition of solid hydridic silicon on the window of the photolysis cell which reduces the light intensity incident on the reactant mixture. This may be seen in Figure 1, in which the relative light intensity incident on N_2O is plotted as a function of the time that the window has been exposed to SiH_4 photodecomposition. As a result of the reduction of light intensity by the solid, it was necessary to make actinometry measurements prior to every SiH_4 photodecomposition experiment. As seen in Figure 1, the rate of solid deposition increases with increasing SiH_4 partial pressure. This necessitated a cleaning of the window after every photolysis of SiH_4 in the few experiments conducted at 8 Torr partial pressure. The formation of solid hydridic silicon also led initially to a frequent plugging of the pinhole leading to the ionization chamber of the mass spectrometer. It was found that this could be greatly minimized simply by packing a small amount of quartz wool around the pinhole.

The photolyses were carried out with SiH_4 at partial pressures of 1–8 Torr in the reaction cell with He used as a diluent gas. At these partial pressures of SiH_4 light absorption is effectively complete. Total pressures in the cell were 42 ± 2 Torr.

SiH_4 was obtained from the Matheson Co., purified by vacuum distillation, and stored in a reservoir on the vacuum line. SiD_4 was prepared by the reduction of $SiCl_4$ (Peninsular Chemical Co.) with $LiAlD_4$ (Alfa Inorganics) and also stored in a glass reservoir. Si_2H_6 was preparaed by the reduction of Si_2Cl_6 with $LiAlH_4$ using bis[2-(2-methoxyethoxy)ethyl] ether as solvent. When the gases formed in this reduction were separated on the vacuum line, it was found that the Si_2H_6 fraction contained SiH_3Cl as an impurity. This impurity was satisfactorily removed by treating the evolved gases again with $LiAlH_4$. Si_3H_8 was prepared from SiH_4 using the electric-discharge method described by Spanier and MacDiarmid.[28] SiH_4 and H_2 were removed from the discharge products by repeated freeze-pump-thaw cycles at −131 °C (*n*-pentane slush bath). Si_2H_6 was separated from the mixture and collected by the same freeze-pump-thaw technique

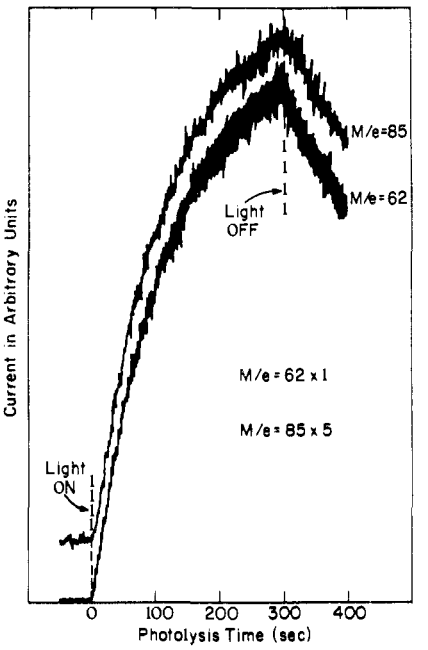

Figure 2. Formation of Si_2H_6 (*m/e* 62) and Si_3H_8 (*m/e* 85) in the photolysis of SiH_4.

at −95 °C (toluene slush bath). Finally Si_3H_8 was removed and collected by several freeze-pump-thaw cycles at −63 °C (chloroform slush bath). Mass spectrometric analyses of the Si_3H_8 before and after a final freeze-pump-thaw cycle gave identical results which were in agreement with the spectrum reported by Pupezin and Zmbov.[29] N_2O and CO_2 were obtained from the Matheson Co. and these gases along with the purified SiH_4 and SiD_4 were subjected to at least one freeze-pump-thaw cycle immediately before use. High-purity grade He, obtained also from Matheson, was used as received, All gas mixtures were prepared using a Saunders-Taylor apparatus.[30]

Results

1. General Nature of the Photodecomposition. Examination of the mass spectra of the contents of the photolysis cell as a function of photolysis time indicates that the products of the photodecomposition of SiH_4 at 147 nm are H_2, Si_2H_6, Si_3H_8, and a solid polymeric film of silicon hydride. Moreover, as can be seen from Figure 2, in which the ion currents of $Si_2H_6^+$ ($i_{62} \propto [Si_2H_6]$) and Si_3H^+ ($i_{85} \propto [Si_3H_8]$) are plotted as a function of photolysis time, Si_3H_8 is not a secondary product but rather a primary product that is formed simultaneously with Si_2H_6. Trace amounts of silanes higher than Si_3H_8 may have been formed but the amounts are just on the limit of our detection sensitivity.

2. Quantum Yields. The quantum yield for the loss of SiH_4 was determined at each partial pressure of SiH_4 from replicate measurements of the initial rates of depletion of SiH_4 in photolyses carried out immediately after an actinometric measurement of the incident light intensity. The initial rates of depletion of SiH_4 and the actinometer gas were determined from the initial rates of decrease of the ion currents of SiH_3^+ (*m/e* 31) and N_2O^+ and/or CO_2^+ (*m/e* 44), respectively, using the relationship[31]

$$-\left(\frac{d[SiH_4]}{dt}\right)_0 = -\frac{[SiH_4]_0}{i_{31^0}}\left(\frac{di_{31}}{dt}\right)_0 \qquad (I)$$

and an analogous expression for the actinometer gas. In (I), $i_{31}{}^0$ is the current of SiH_3^+ (*m/e* 31) before the photolysis is begun, $[SiH_4]_0$ is the initial concentration, and the subscripts to the parenthetical terms denote initial rates. Note from (I) that the initial rates of depletion of reactants may be obtained without prior calibration of the mass spectrometer. Typical recorder tracings from which the initial slopes $(di_{31}/dt)_0$ and

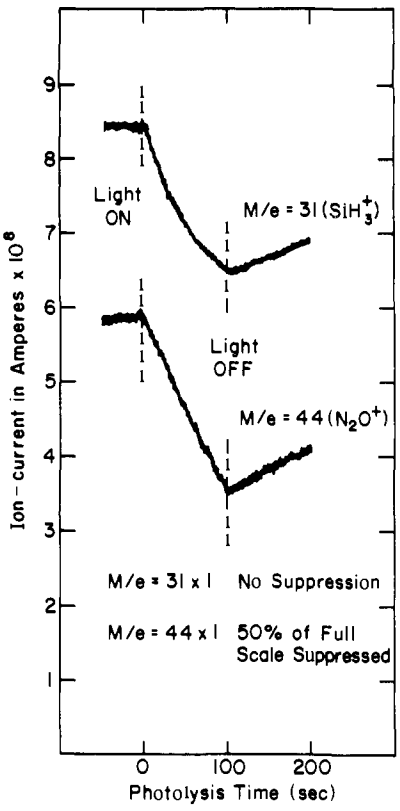

Figure 3. Typical depletion curve obtained in the determination of the quantum yield $\Phi(-SiH_4)$, SiH_4 (*m/e* 31) and actinometer gas, N_2O (*m/e* 44).

$(di_{44}/dt)_0$ were calculated are shown in Figure 3. Since the absorption coefficients of the actinometer gases are known,[32,33] the observed rates of depletion of N_2O and CO_2 are readily combined with the known quantum yields[14-23] to compute the light intensity, I_0, incident on the contents of the photolysis cell. The absorption coefficient of SiH_4 is likewise known[25] and, hence, the quantum yield of SiH_4 photodecomposition was computed from the rate data using the expression

$$\Phi(-SiH_4) = -\left(\frac{d[SiH_4]}{dt}\right)_0 \left(\frac{V}{I_0}\right)(1 - e^{-\alpha[SiH_4]_0 L})^{-1} \quad \text{(II)}$$

In (II) V and L are the volume and length, respectively, of the photolysis cell, α is the absorption coefficient of SiH_4 for 147-nm radiation, and the other terms are as described previously. There are small additional contributions to *m/e* 31 due to the SiH_3^+ formed in the electron impact dissociation of the products, Si_2H_6 and Si_3H_8. As a result the rate (di_{31}/dt) in (I) must be corrected for increases due to formation of these products before calculation of $\Phi(-SiH_4)$ by (II). The correction, which is easily made from the mass spectra of pure SiH_4, Si_2H_6, and Si_3H_8 and from the initial rates $-(di_{31}/dt)_0$, $(di_{62}/dt)_0$, and $(di_{85}/dt)_0$, amounts to about 10%.

The quantum yields for formation of Si_2H_6 and Si_3H_8 were obtained from the known absorbed light intensity and initial slopes using the relationships

$$\left(\frac{di_{62}}{dt}\right)_0 = \beta_{62}\left(\frac{d[Si_2H_6]}{dt}\right)_0 \quad \text{(III)}$$

$$\left(\frac{di_{85}}{dt}\right)_0 = \beta_{85}\left(\frac{d[Si_3H_8]}{dt}\right)_0 \quad \text{(IV)}$$

where β_{62} and β_{85} use the mass spectrometric calibration factors relating ion currents at the given *m/e* to concentrations of the parent molecules. In the case of the reaction products, it was thus necessary to calibrate the mass spectrometer with samples of pure Si_2H_6 and Si_3H_8.

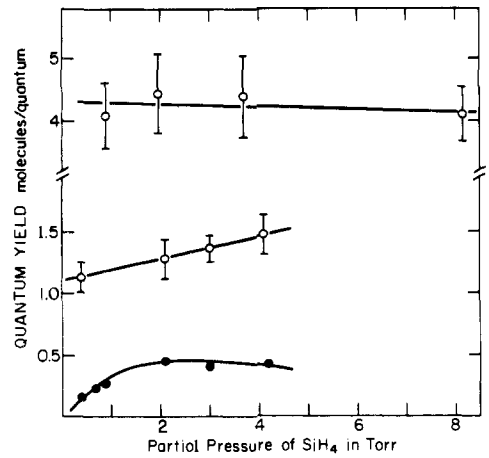

Figure 4. Dependence of quantum yields on the partial pressure of SiH_4.

Table I. Quantum Yields in the Photodecomposition of SiH_4 at 147 nm[a]

reactive gas	partial pressure, Torr	$\Phi(-SiH_4)$	$\Phi(Si_2H_6)$	$\Phi(Si_3H_8)$
SiH_4	0.4		1.14 ± 0.05	0.16 ± 0.02
SiH_4	0.7			0.24 ± 0.02
SiH_4	0.9	4.1 ± 0.5		0.27 ± 0.02
SiH_4	2.1	4.4 ± 0.6	1.29 ± 0.08	0.46 ± 0.01
SiH_4	3.0		1.37 ± 0.05	0.41 ± 0.02
SiH_4	3.7	4.4 ± 0.7		
SiH_4	4.1		1.48 ± 0.08	0.43 ± 0.02
SiH_4	8.1	4.1 ± 0.4		
SiD_4	2.0	4.4 ± 0.2		

[a] Diluent gas = He; total pressure = 42 Torr.

The quantum yields for the decomposition of SiH_4 and for the formation of Si_2H_6 and Si_3H_8 are shown in Table I. Each quantum yield in the table is the mean of three to eight replicate experiments and the uncertainties indicated are the average deviations from the mean. Considerably greater uncertainties are associated with the quantum yields for destruction of SiH_4 because the determination of initial slopes for loss of reactant involves small differences between relatively large numbers. Measurement of $\Phi(H_2)$ was not feasible in our apparatus. The dependence of the quantum yields on the partial pressure of SiH_4 is shown in Figure 4.

According to these data, more than four molecules of SiH_4 are decomposed per quantum absorbed and the quantum yield is only slightly dependent on the partial pressure of SiH_4 in the range of 0.9-8.1 Torr. The apparent slight decrease in $\Phi(-SiH_4)$ with increasing partial pressure of SiH_4 is just within the experimental uncertainty and so we cannot be sure that it is real. However, the direction of the slight dependence of $\Phi(-SiH_4)$ on $[SiH_4]$ is consistent with the expectations from the mechanism to be discussed later. The values of $\Phi(-SiH_4)$ were determined at various stages of the buildup of the solid silicon hydride, for a given partial pressure of $[SiH_4]$, and, therefore, at light intensities that were reduced by up to a factor of 6 from that characteristic of a freshly cleaned window (cf. Figure 1). The quantum yields obtained showed no observable trend from the average values shown in Table I. We conclude, therefore, that $\Phi(-SiH_4)$ is independent of light intensity over a sixfold variation and is independent of the amount of solid silicon hydride present on the surfaces of the photolysis cell. As may be seen in Table I, the quantum yield for photodecomposition of monosilane is independent of deuterium substitution, i.e., $\Phi(-SiH_4) = \Phi(-SiD_4)$.

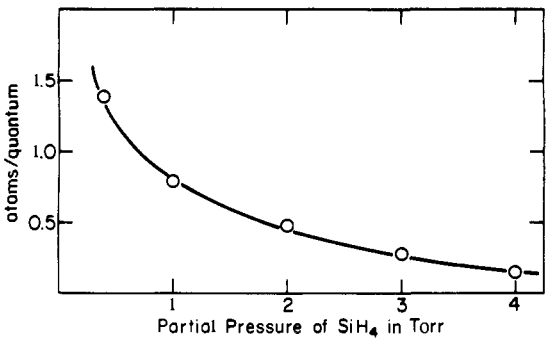

Figure 5. Quantum yield for silicon atoms appearing in solid film as a function of partial pressure of SiH_4.

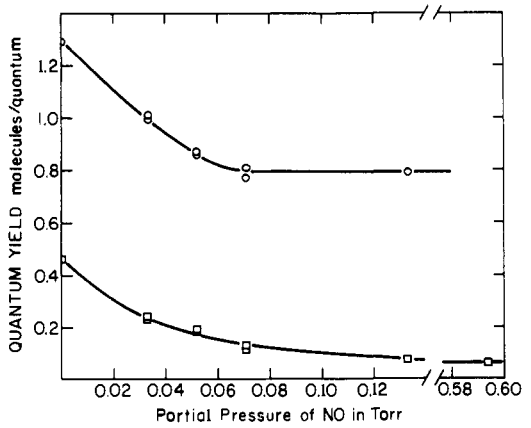

Figure 6. Dependence of quantum yields for Si_2H_6 and Si_3H_8 formation on partial pressure of NO. Initial $P(SiH_4)$ = 2 Torr: ○, Si_2H_6; □, Si_3H_8.

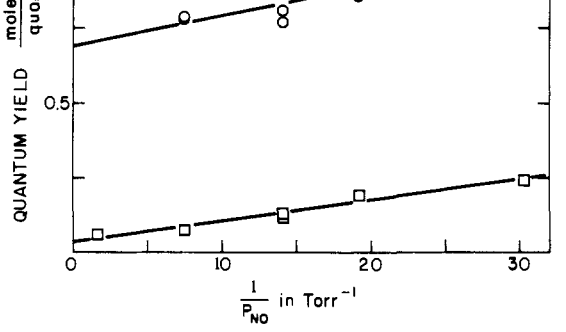

Figure 7. Extrapolation of quantum yields to conditions of complete monovalent-radical interception by NO. Initial $P(SiH_4)$ = 2 Torr.

The quantum yield for Si_2H_6 formation increases with increasing partial pressure of SiH_4 from an apparent low-pressure limit of slightly more than unity to a value of 1.5 at 4 Torr. The apparent linear increase in $\Phi(Si_2H_6)$, shown in Figure 4, cannot continue indefinitely with increasing pressure, because conservation of matter requires $\Phi(Si_2H_6) < \frac{1}{2}\Phi(-SiH_4)$. In view of the dependence of $\Phi(-SiH_4)$ on partial pressure of SiH_4 (cf. Figure 3), the upper limit of $\Phi(Si_2H_6)$ appears to be ~2. The quantum yield for formation of Si_3H_8 depends quite differently on pressure than does $\Phi(Si_2H_6)$. Thus, as shown in Figure 4, $\Phi(Si_3H_8)$ increases with increasing $P(SiH_4)$ from a low-pressure limit of zero to an apparent broad maximum at about 2 Torr. The data in Figure 4 cannot differentiate between a broad maximum or a plateau in $\Phi(Si_3H_8)$. However, the dependencies of $\Phi(-SiH_4)$ and $\Phi(Si_2H_6)$ on $P(SiH_4)$ and the conservation of mass require this to be a maximum.

Material balances on silicon, based on the data in Table I and in Figure 3, indicate that the gaseous products Si_2H_6 and Si_3H_8 account for about 68% of the SiH_4 that has reacted at $P(SiH_4)$ = 0.5 Torr but for nearly 100% of the reacted SiH_4 at $P(SiH_4)$ = 4 Torr. Quantum yields for Si atoms appearing in the solid film, as calculated from the material balances, are shown as a function of $P(SiH_4)$ in Figure 5.

3. Effect of Nitric Oxide on Quantum Yields. Nitric oxide was added to the photolysis system, at partial pressures such that its light absorption was negligible, in order to intercept and thereby suppress the reactions of monovalent radicals. It has been shown, for example, that divalent silylene radicals such as SiH_2 and CH_3SiH are unreactive toward NO[3] but that monovalent radicals such as SiH_3 and CH_3SiH_2 are very effectively scavenged[9,10] from the system by NO.

The effect of NO addition on the quantum yields for formation of Si_2H_6 and Si_3H_8, in the photolysis of SiH_4 at 2.1 Torr, are shown in Figure 6. The quantum yields of both Si_2H_6 and Si_3H_8 are reduced by increasing partial pressures of NO but the effectiveness of the suppression is clearly greater for $\Phi(Si_3H_8)$ than for $\Phi(Si_2H_6)$. The limiting values of $\Phi(Si_2H_6)$ and $\Phi(Si_3H_8)$ under conditions of complete suppression of monovalent radical sources may be determined as the intercepts of plots of quantum yields vs. the reciprocal of the NO partial pressure. Such plots, which are shown in Figure 7, indicate that under complete monovalent radical scavenging conditions $\Phi(Si_2H_6)$ is reduced to 53% of the unscavenged value, while the corresponding percentage for $\Phi(Si_3H_8)$ is 7%.

The presence of NO results in an increase in the quantum yield for depletion of SiH_4 from 4.4 (cf. Table I) to ~7 and in the formation of the additional products N_2O, SiH_3OSiH_3, and $(SiH_3O)_2SiH_2$. This was expected because it has been shown[9,10,34] that the generation of SiH_3 radicals in the presence of SiH_4 and NO initiates a chain reaction that consumes NO and SiH_4 on an approximately 1:1 basis with the formation of N_2O and the siloxanes. Quantum yields for the depletion of NO and for the formation of N_2O and the siloxanes by this known chain process were not measured.

Discussion

1. Nature of the Reaction Intermediates. A previous investigation[10] of the $Hg(^3P_1)$-photosensitized decomposition of SiH_4 showed the suppression of Si_2H_6 formation by NO to be complete and to be accompanied by the formation of SiH_3OSiH_3 and higher siloxanes. It was, therefore, concluded that in the $Hg(^3P_1)$-photosensitized decomposition of SiH_4 all of the Si_2H_6 arises from SiH_3 radicals.[10] This means that the primary process, namely, the collision of $Hg(^3P_1)$ atoms with SiH_4 molecules, produces predominantly SiH_3 radicals and H atoms.

In the present case, with 147-nm radiation, the situation is quite different. As shown in Figures 6 and 7, the suppression of Si_3H_8 appears to be nearly complete but that of Si_2H_6 is definitely not. The partial suppression by NO and the observation of SiH_3OSiH_3 as a product indicate that SiH_3 radicals are intermediates. However, the fact that the reduction of $\Phi(Si_2H_6)$ and $\Phi(Si_3H_8)$ by NO is not complete but is rather only 47 and 93%, respectively, indicates the presence of at least one other reactive intermediate. This intermediate must be one that leads to both Si_2H_6 and Si_3H_8 but is unreactive toward NO. In this respect the 147-nm photolysis is very similar to the γ-ray radiolysis of SiH_4 in the presence of NO, because in this case suppression of Si_2H_6 formation by NO is also not complete.[34] However, unlike the radiolysis, in the 147-nm photolysis there is not sufficient energy to generate the ionic species SiH_3^+, which leads ultimately to Si_2H_6 and which is unreactive

toward NO. The most obvious intermediate that can be formed in the photolysis that is unreactive toward NO but that will form Si_2H_6 by insertion into the Si–H bonds of SiH_4 is the singlet diradical SiH_2. The insertion reaction of SiH_2 with SiH_4 has been well established[35] and, moreover, SiH_2 and CH_3SiH have been shown to be important intermediates in the 147-nm photolysis of CH_3SiH_3 and to be unreactive toward NO.[3] In order to form Si_3H_8 simultaneously with Si_2H_6, in the presence and absence of NO, it is necessary to postulate the presence of a divalent radical that will insert into the Si–H bonds to form Si_3H_8. The most likely candidate for such a reaction is the SiH_3SiH radical, a species suggested by Pollock, Sandhu, Jodhan, and Strausz.[36]

On the basis of the above discussion we conclude that SiH_2, SiH_3, SiH_3SiH, and H atoms are major reactive intermediates in the 147-nm photolysis of SiH_4. Energetically, it is possible that other silicon-containing species such as SiH and Si could be formed by dissociation of photoactivated SiH_4 molecules. We have no evidence for or against their presence. However, as will be seen, it is not necessary to invoke the presence of such species to explain our experimental results and, on these grounds, we assume that SiH and Si are not present in significant amounts.

2. Mechanism of the Photolysis. Any proposed mechanism must account for and be consistent with the following facts that were presented in a previous section.

(1) More than four molecules of SiH_4 are reacted per quantum of light absorbed (cf. Table I and Figure 4).

(2) Si_2H_6 and Si_3H_8 are formed simultaneously as primary products (cf. Figure 2).

(3) The quantum yield of Si_2H_6 has an apparently finite value in the limit of zero partial pressure of SiH_4 but that of Si_3H_8 is zero.

(4) The quantum yields are independent of light intensity over a sixfold range.

(5) Complete interception of monovalent free radicals by NO suppresses partially but not completely the quantum yields of Si_2H_6 and Si_3H_8. The suppression by NO is much more effective for $\Phi(Si_3H_8)$ than for $\Phi(Si_2H_6)$.

After consideration of a number of possible mechanisms, we propose that shown by (1)–(14) to represent the most satisfactory description of the 147-nm photolysis of SiH_4.

$$SiH_4 + h\nu \rightarrow SiH_2 + 2H \quad (1A)$$

$$SiH_4 + h\nu \rightarrow SiH_3 + H \quad (1B)$$

$$H + SiH_4 \rightarrow H_2 + SiH_3 \quad (2)$$

$$SiH_3 + SiH_3 \rightarrow SiH_4 + SiH_2 \quad (3)$$

$$SiH_3 + SiH_3 \rightarrow Si_2H_6{}^{**} \quad (4)$$

$$Si_2H_6{}^{**} \rightarrow SiH_4 + SiH_2 \quad (5)$$

$$Si_2H_6{}^{**} \rightarrow H_2 + SiH_3SiH \quad (6)$$

$$Si_2H_6{}^{**} + M \rightarrow Si_2H_6 + M \quad (7)$$

$$SiH_2 + SiH_4 \rightarrow Si_2H_6{}^{*} \quad (8)$$

$$Si_2H_6{}^{*} \rightarrow H_2 + SiH_3SiH \quad (9)$$

$$Si_2H_6{}^{*} + M \rightarrow Si_2H_6 + M \quad (10)$$

$$SiH_3SiH \rightarrow \cdot SiH_2SiH_2 \cdot \quad (11)$$

$$SiH_3SiH + SiH_4 \rightarrow Si_3H_8 \quad (12)$$

$$SiH_3 + \text{wall} \rightarrow \text{solid} \quad (13)$$

$$\cdot SiH_2SiH_2 \cdot + \text{wall} \rightarrow \text{solid} \quad (14)$$

The reaction denoted as (1A) is most probably the predominant primary process because, unless some hitherto unknown chain reaction is operating or unless hitherto unknown reactions of SiH are invoked, it is the only primary process that can account for the fact that more than four molecules of SiH_4 are reacted per quantum absorbed. Secondly, by itself, it accounts very nearly for the fact (cf. Figures 6 and 7) that the sum of the quantum yields, $\Phi(Si_2H_6) + \Phi(Si_3H_8)$, is reduced by NO to a little more than $\frac{1}{2}$ of the value observed in the absence of NO. Thus, each H atom formed produces an SiH_3 radical by (2) and, if the surface reaction (13) and isomerization reaction (11) are neglected, each pair of SiH_3 radicals forms either Si_2H_6 or Si_3H_8. Interception of SiH_3 by NO will cause a reduction in the sum of yields, $\Phi(Si_2H_6) + \Phi(Si_3H_8)$, resulting from (1A) to $\frac{1}{2}$ of the value that would be observed in the absence of NO.

Inspection of Figures 6 and 7 indicates that the sum, $\Phi(Si_2H_6) + \Phi(Si_3H_8)$, is actually suppressed by NO to 0.42 of the value observed in the absence of NO. This means that an additional primary process is required and this process must be one that yields products that can all be intercepted by NO. The only feasible reaction that meets these characteristics is (1B). Since, under conditions of complete monovalent radical suppression, (1B) cannot contribute at all to Si_2H_6 and Si_3H_8 formation and (1A) is reduced to $\frac{1}{2}$ of its effectiveness, the data in Figures 6 and 7 lead to the following primary quantum yields:

$$\phi_{1A} = 0.83$$

$$\phi_{1B} = 0.17$$

The occurrence of a primary process that yields the products $SiH_2 + H_2$, a process that is analogous to what has been proposed for CH_4,[37] cannot be ruled out completely. However, the products of this reaction cannot be intercepted by NO. Secondly, such a primary process would lead to a value of $\Phi(-SiH_4)$ of between 2 and 3. In view of the above discussion, such a primary process could play only a very minor role in the photolysis of SiH_4.

The reaction of H atoms with SiH_4 is very rapid[31] and there is no question that at the pressures employed in this work all H atoms will react by (2).

Two separate processes, namely, (3) and (4), are written for the bimolecular reaction of SiH_3 radicals on the basis of the work of Reimann, Matten, Laupert, and Potzinger.[38] By pressure-dependence studies of the products formed by reactions of SiH_3 with SiD_3 radicals, these authors[38] demonstrated the existence of the two separate pathways, (3) and (4), with $k_3/k_4 = 0.7$ at 300 K. The same authors also demonstrated the occurrence of (5) and (7). In reactions (4)–(7) the symbol $Si_2H_6{}^{**}$ indicates an activated disilane molecule that has an internal excitation energy of 73 kcal/mol because it has been formed by the combination of SiH_3 radicals.[39]

Reaction 8 has been well established[35] though it is not usually written in this form. The symbol $Si_2H_6{}^{*}$ indicates an activated disilane molecule with an excess energy of 49 kcal/mol.[35] Reactions 6 and 12 are based on our observation of simultaneous Si_2H_6 and Si_3H_8 formation, on the known tendency of silylene-type diradicals to insert into Si–H bonds, and on the fact that $\Phi(Si_3H_8)$ is not reduced to zero by NO.

The decomposition and stabilization reactions of $Si_2H_6{}^{*}$, namely, (9) and (10), are written to account for the fact that, even though SiH_3 radicals are completely intercepted by NO, the quantum yield $\Phi(Si_3H_8)$ is still finite in the limit of total scavenging. Bond-energy considerations[39] suggest that (9) is exothermic to the extent of 1–2 kcal. Reaction 11 is included on the basis of a suggestion by Pollack, Sandhu, Jodhan, and Strausz[36] made in their report on the $Hg(^3P_1)$-photosensitized decomposition of Si_2H_6.

Finally, reactions 13 and 14 are included to account for the formation of solid silicon hydride on the surfaces of the vessel.

3. Kinetic Treatment of the Mechanism. At partial pressures of SiH_4 of 1 Torr and above, the products Si_2H_6 and Si_3H_8 account for at least 81% of the Si atoms that have reacted. Therefore, for pressures above 1 Torr, it is a reasonable approximation to neglect the surface reactions (13) and (14) in deriving expressions for the steady-state concentrations of reactive transients. A standard steady-state treatment of (1)-(12) leads in a straightforward manner to the following expressions for the overall quantum yields.

$$\phi(-SiH_4) = 2(2\phi_{1A} + \phi_{1B}) + \frac{k_{12}[SiH_4]}{k_{11} + k_{12}[SiH_4]} \times \left\{\frac{k_9}{k_9 + k_{10}[M]}\left(\phi_{1A} + \frac{k_3}{k_3 + k_4} + \frac{k_4}{k_3 + k_4} \times \frac{k_5}{k_5 + k_6 + k_7[M]}\right) + \frac{k_4}{k_3 + k_4}\frac{k_6}{k_5 + k_6 + k_7[M]}\right\} \quad (V)$$

$$\Phi(Si_2H_6) = \frac{k_{10}[M]}{k_9 + k_{10}[M]}\left\{\phi_{1a} + \frac{k_3}{k_3 + k_4} + \frac{k_4}{k_3 + k_4} \times \frac{k_5}{k_5 + k_6 + k_7[M]}\right\} + \frac{k_4}{k_3 + k_4}\frac{k_7[M]}{k_5 + k_6 + k_7[M]} \quad (VI)$$

$$\Phi(Si_3H_8) = \frac{k_{12}[SiH_4)}{k_{11} + k_{12}[SiH_4]}\left\{\frac{k_4}{k_3 + k_4}\frac{k_6}{k_5 + k_6 + k_7[M]} + \frac{k_9}{k_9 + k_{10}[M]}\left(\phi_{1A} + \frac{k_3}{k_3 + k_4} + \frac{k_4}{k_3 + k_4} \times \frac{k_5}{k_5 + k_6 + k_7[M]}\right)\right\} \quad (VII)$$

In the expressions (V)-(VII), the general deactivation terms $k_7[M]$ and $k_{10}[M]$ denote the sums $k_7[He] + k_7'[SiH_4]$ and $k_{10}[He] + k_{10}'[SiH_4]$, respectively.

The cumbersome expressions in (V)-(VII) show that the mechanism predicts the quantum yields to be independent of light intensity. However, they can be simplified somewhat by consideration of some experimental facts. Firstly, the fact that $\Phi(-SiH_4)$ and $\Phi(Si_3H_8)$ both decrease with increasing partial pressure of SiH_4 above 2 Torr indicates that $k_{12}[SiH_4] \gg k_{11}$. Secondly, combination of this fact with the observation that $\Phi(Si_3H_8)$ under complete scavenging conditions is only 0.07 of its value in the absence of NO leads to the conclusion that $k_{10}[M] = 13k_9$, i.e., $k_{10}[M] \gg k_9$ is a reasonable approximation. The fact that $k_{10}[M] \gg k_9$ is in accord with the thermochemical estimate that the excitation energy in Si_2H_6* that must be removed amounts to only 1.3 kcal/mol[35] and collisional stabilization should be very rapid. Substitution of these approximations into the expressions in (V), (VI), and (VII) yields the simplified predictions by the mechanism for the quantum yields above 2 Torr of SiH_4 that are shown in (VIII), (IX), and (X).

$$\Phi(-SiH_4) \approx 2(2\phi_{1A} + \phi_{1B}) + \left(\frac{k_4}{k_3 + k_4}\right)\left(\frac{k_6}{k_5 + k_6 + k_7[M]}\right) \quad (VIII)$$

$$\Phi(Si_2H_6) \approx \phi_{1A} + \frac{k_3}{k_3 + k_4} + \left(\frac{k_4}{k_3 + k_4}\right)\left(\frac{k_5 + k_7[M]}{k_5 + k_6 + k_7[M]}\right) \quad (IX)$$

$$\Phi(Si_3H_8) \approx \left(\frac{k_4}{k_3 + k_4}\right)\left(\frac{k_6}{k_5 + k_6 + k_7[M]}\right) \quad (X)$$

According to these approximations, the sum of (IX) and (X) should be

$$\Phi(Si_2H_6) + \Phi(Si_3H_8) \approx \Phi_{1A} + 1 = 1.83$$

which is in excellent agreement with the experimental values of $\Phi(Si_2H_6) + \Phi(Si_3H_8)$ at 2, 3, and 4 Torr, namely, 1.75, 1.78, and 1.91 (cf. Table I). Reimann, Matten, Laupert, and Potzinger[38] have reported that $k_3/k_4 = 0.7$, which means that the fractions $k_3/(k_3 + k_4)$ and $k_4/(k_3 + k_4)$ have the values of 0.41 and 0.59, respectively. Using these values and the experimental results for $\Phi(Si_3H_8)$ (cf. Table I) we obtain at a partial pressure of SiH_4 of 2.1 Torr the result

$$\frac{k_6}{k_5 + k_6 + k_7[M]} = 1 - \frac{k_5 + k_7[M]}{k_5 + k_6 + k_7[M]} = 0.78 \quad (XI)$$

which means that most of the highly energized Si_2H_6** molecules dissociate via (6) before being stabilized. Insertion of the result in (XI) into the expressions in (VIII) and (IX) then gives for the predicted quantum yields the values

$$\Phi(-SiH_4) \approx 4.1 \quad (XII)$$

$$\Phi(Si_2H_6) \approx 1.37 \quad (XIII)$$

The predicted quantum yields in (XII) and (XIII) are in agreement with the data in Table I, within the experimental error. Considering the complexity of the reaction and the approximations used to obtain (VIII), (IX), and (X), this is satisfactory agreement. Thus, the proposed mechanism is not only in accord with our own results but is consistent with the results of Reimann, Matten, Laupert, and Potzinger.[38]

The decrease of $\Phi(-SiH_4)$ with increasing partial pressure of SiH_4 (cf. Figure 4) is accounted for by (VIII) since $k_7[M] = k_7[He] + k_7'[SiH_4]$. The linear increase of $\Phi(Si_2H_6)$ with increasing partial pressure of SiH_4 is accounted for by (IX), since, as we have shown, $k_6 \gg k_5 + k_7[M]$. The decrease of $\Phi(Si_3H_8)$ toward zero can only be accounted for by the full expression, (VII), under conditions that $k_{12}[SiH_4] \ll k_{11}$.

At very low pressures of SiH_4, the rate of absorption of light and, therefore, the rate of formation of SiH_3 radicals will be greatly reduced. This means that at low SiH_4 pressure the wall reaction of SiH_3 radicals will become dominant in determining the steady-state concentration of SiH_3 radicals. The mechanism will thus change somewhat and the expressions (V)-(X) will no longer be strictly valid. It should be mentioned that, although the complete expressions (VI) and (VII) predict a finite low-pressure limit for $\Phi(Si_2H_6)$, this is only an apparent limit that results from the absence in the mechanism of reaction channels for SiH_2 other than (8). Clearly in the limit of zero pressure SiH_2 cannot react with SiH_4 and $\Phi(Si_2H_6)$ must go to zero. However, (8) is sufficiently fast[35] that a decrease in $\Phi(Si_2H_6)$ will not be observable at the partial pressures of SiH_4 used in our work.

4. Formation of Solid Film. Consideration of the known rate constant of (8), and the assumption that (12) is comparable to (8), leads one to conclude that the only reaction transients reaching the walls of the vessel are SiH_3 and SiH_2SiH_2 radicals. We think, therefore, that the wall reactions of these entities are responsible for the buildup of polymeric silicon hydride. The dependence of the quantum yield for adsorbed Si atoms as a function of the partial pressure of SiH_4 (cf. Figure 5) shows that $\Phi(Si_{wall})$ decreases as $P(SiH_4)$ is increased. The proposed mechanism is consistent with this fact in that it predicts the probability of (3) and (4) relative to (13) and of (12) relative to (11) to increase with increasing partial pressure of SiH_4.

Acknowledgment. This work was supported by the U.S. Department of Energy under Contract EY-76-S-02-3416.

References and Notes

(1) Department of Energy Document No. EY-76-S-02-3416-7.
(2) O. P. Strausz, K. Obi, and W. K. Duholke, *J. Am. Chem. Soc.*, **90**, 1359 (1968).
(3) K. Obi, A. Clement, H. E. Gunning, and O. P. Strausz, *J. Am. Chem. Soc.*, **91**, 1622 (1969).
(4) A. G. Alexander and O. P. Strausz, *J. Phys. Chem.*, **80**, 2531 (1976).

(5) M. A. Ring, G. D. Beverly, F. H. Koester, and R. P. Hollandsworth, *Inorg. Chem.*, **8**, 2033 (1969).
(6) H. J. Emeleus and R. Stewart, *Trans. Faraday Soc.*, **32**, 1577 (1936).
(7) D. White and E. G. Rochow, *J. Am. Chem. Soc.*, **76**, 3987 (1954).
(8) H. Niki and G. J. Mains, *J. Phys. Chem.*, **68**, 304 (1964).
(9) M. S. Nay, G. N. C. Woodall, O. P. Strausz, and H. E. Gunning, *J. Am. Chem. Soc.*, **87**, 179 (1965).
(10) E. Kamaratos and F. W. Lampe, *J. Phys. Chem.*, **74**, 2267 (1970).
(11) E. R. Austin and F. W. Lampe, *J. Phys. Chem.*, **80**, 2811 (1976).
(12) B. Reimann, A. Matten, R. Laupert, and P. Potzinger, *Ber. Bunsenges. Phys. Chem.*, **81**, 500 (1977).
(13) R. Gorden, R. E. Rebbert, and P. Ausloos, *Natl. Bur. Stand. (U.S.), Tech. Note*, **No. 496** (1969).
(14) W. Groth, *Z. Phys. Chem., Abt. B*, **37**, 307 (1937).
(15) B. H. Mahan, *J. Chem. Phys.*, **33**, 959 (1960).
(16) J. Y. Yang and F. M. Servedio, *Can. J. Chem.*, **46**, 338 (1968).
(17) L. J. Stief, V. J. DeCarlo, and W. A. Payne, *J. Chem. Phys.*, **51**, 3336 (1969).
(18) T. G. Slanger and G. Black, *J. Chem. Phys.*, **54**, 1889 (1971).
(19) T. G. Slanger, R. L. Sharples, G. Black, and S. V. Filseth, *J. Chem. Phys.*, **61**, 5022 (1974).
(20) M. Zelikoff and L. M. Aschenbrand, *J. Chem. Phys.*, **22**, 1680 (1954).
(21) W. E. Groth and H. Schierholz, *Planet. Space Sci.*, **1**, 333 (1959).
(22) J. Y. Yang and F. M. Servedio, *J. Chem. Phys.*, **47**, 4817 (1967).
(23) M. C. Dodge and J. Heicklen, *Int. J. Chem. Kinet.*, **3**, 269 (1971).
(24) G. G. A. Perkins, E. R. Austin, and F. W. Lampe, *J. Chem. Phys.*, **68**, 4357 (1978).
(25) Y. Harada, J. N. Murrel, and H. H. Sheena, *Chem. Phys. Lett.*, **1**, 595 (1968).
(26) H. Okabe and D. A. Becker, *J. Chem. Phys.*, **39**, 2545 (1963).
(27) J. G. Calvert and J. N. Pitts, Jr., "Photochemistry", Wiley, New York, 1966, p 493.
(28) E. J. Spanier and A. G. MacDiarmid, *Inorg. Chem.*, **1**, 432 (1962).
(29) J. D. Pupezin and K. F. Zmbov, *Bull. Inst. Nucl. Sci. "Boris Kidrich"*, **8**, 89 (1958).
(30) K. W. Saunders and H. A. Taylor, *J. Chem. Phys.*, **9**, 616 (1941).
(31) E. R. Austin and F. W. Lampe, *J. Phys. Chem.*, **81**, 1134 (1977).
(32) M. Zelikoff, K. Watanabe, and E. C. Y. Inn, *J. Chem. Phys.*, **21**, 1643 (1953).
(33) E. C. Y. Inn, K. Watanabe, and M. Zelikoff, *J. Chem. Phys.*, **21**, 1648 (1953).
(34) J. P. Bare and F. W. Lampe, *J. Phys. Chem.*, **81**, 1437 (1977).
(35) P. John and J. H. Purnell, *J. Chem. Soc., Faraday Trans. 1*, **69**, 1455 (1973).
(36) T. L. Pollock, H. S. Sandhu, A. Jodhan, and O. P. Strausz, *J. Am. Chem. Soc.*, **95**, 1017 (1973).
(37) Reference 27, p 498.
(38) B. Reimann, A. Matthen, R. Laupert, and P. Potzinger, *Ber. Bunsenges. Phys. Chem.*, **81**, 500 (1977).
(39) P. Potzinger, A. Ritter, and J. Krause, *Z. Naturforsch. A*, **30**, 347 (1975).

Stereochemistry and Stereochemical Rearrangements of Eight-Coordinate Tetrakis Chelates. 1. Group 4B β-Diketonates[1]

Robert C. Fay* and John K. Howie

Contribution from the Department of Chemistry, Cornell University, Ithaca, New York 14853. *Received August 13, 1978*

Abstract: Until very recently, NMR studies of eight-coordinate tetrakis chelates have failed to provide stereochemical and kinetic information because these chelates undergo very rapid stereochemical rearrangements. Using the Freon solvent $CHClF_2$, the ^1H and ^{19}F NMR spectra of Zr(IV), Hf(IV), Ce(IV), and Th(IV) tetrakis(β-diketonates) have been investigated at considerably lower temperatures than employed in earlier work, and several complexes have been identified which become stereochemically rigid on the NMR time scale at temperatures in the range −115 to −170 °C. The spectra of $Zr(acac)_4$ and $Hf(acac)_4$ in the slow-exchange limit are most simply interpreted in terms of the presence of a single stereoisomer (*ssss*-D_2, *mmmm*-D_{2d}, *gggg*-D_2, or *gggg*-S_4); the square antiprismatic *ssss*-D_2 configuration is preferred on the basis of the solid-state structure of $Zr(acac)_4$. The alkyl resonances of $Zr(dmh)_4$ and $Zr(tfac)_4$ (dmh = *t*-$C_4H_9COCHCOCH_3^-$; tfac = CF_3CO-$CHCOCH_3^-$) do not probe the overall symmetry of these molecules, only the local site symmetry of the alkyl groups. However, the ^{19}F spectra of $Zr(tfac)_4$ show that more than one geometric isomer is present. The ^1H spectrum of $Zr(acac)_2(NO_3)_2$ is consistent with the *mmmm*-C_2 dodecahedral structure found in the solid state. No splitting of the time-averaged NMR resonances was found for the Ce and Th complexes. The kinetics of the intramolecular rearrangement processes which exchange acac methyl groups or dmh *tert*-butyl groups between the two inequivalent sites of $Zr(acac)_4$, $Zr(acac)_2(NO_3)_2$, and $Zr(dmh)_4$ have been studied by NMR line-shape analysis. Rate constants (s^{-1} at −125 °C), $\Delta H^{\ddagger}$ (kcal/mol), and $\Delta S^{\ddagger}$ (eu) are respectively as follows: 2.0×10^2, 4.1 ± 0.3, and −18.7 ± 2.5 for $Zr(acac)_4$; 2.9×10^2, 4.5 ± 0.3, and −15.2 ± 2.5 for $Zr(acac)_2(NO_3)_2$; 6.8, 5.5 ± 0.5, and −16.2 ± 2.9 for $Zr(dmh)_4$. Polytopal rearrangement, involving a series of Hoard-Silverton rearrangements, is the preferred path for these rearrangements; however, one-bond rupture mechanisms cannot be ruled out.

Introduction

Stereochemical nonrigidity is a characteristic property of eight-coordinate complexes, and until very recently no examples of "stereochemically rigid" tetrakis chelates had been identified. Low-temperature NMR studies of tetrakis β-diketonates,[2,3] tropolonates,[4] and *N,N*-dialkyldithiocarbamates[5-8] had afforded only time-averaged NMR spectra. The first examples of tetrakis chelates which become rigid on the NMR time scale have been reported within the past 3 years. The reported examples are (1) the tetrakis(*N,N*-dimethyldithiocarbamato)tantalum(V) cation, $[Ta(S_2CNMe_2)_4]^+$;[9] (2) the *N,N*-dimethylmonothiocarbamate complexes, $Ti(SOCNMe_2)_4$ and $Zr(SOCNMe_2)_4$;[10] and (3) the W(IV) mixed ligand complexes, $W(mpic)_3(dcq)$ and $W(mpic)_2(dcq)_2$[11] (mpic = 5-methylpicolinate and dcq = 5,7-dichloro-8-quinolinolate). $W(mpic)_2(dcq)_2$ can be separated into two geometric isomers which isomerize slowly on the laboratory time scale; $\Delta G^{\ddagger} = 24.1$ kcal/mol at 25 °C.[11]

Using the Freon solvent $CHClF_2$, we have investigated the ^1H and ^{19}F NMR spectra of Zr(IV), Hf(IV), Ce(IV), and Th(IV) tetrakis(β-diketonates) at considerably lower temperatures than employed in earlier work,[2] and we have identified several complexes which become stereochemically rigid on the NMR time scale at temperatures in the range −115 to −170 °C. In this paper we describe the low-temperature spectra, consider the stereochemistry of these complexes in solution, and discuss the kinetics and mechanism of stereochemical rearrangements. A subsequent paper will deal with the paramagnetic uranium(IV) analogues.

Experimental Section

Reagents and General Techniques. Zirconium(IV) chloride (Chemical Procurement Laboratories), zirconium(IV) isopropoxide

0002-7863/79/1501-1115$01.00/0